Differential Regulation of the Lateral Mobility of Plasma Membrane Phospholipids by the Extracellular Matrix and Cholesterol

O.G. RAMPRASAD,[1] NANDINI RANGARAJ,[1] G. SRINIVAS,[1] JEAN PAUL THIERY,[2] SYLVIE DUFOUR,[2] AND GOPAL PANDE[1]*

[1]*Center for Cellular and Molecular Biology, Hyderabad, India*

[2]*UMR 144 CNRS-Institut Curie, Paris, France*

In this study, we compared qualitative and quantitative changes in the lateral mobility of phospholipid molecules in the plasma membrane of intact cells under various conditions of specific interaction of integrins in the cell membrane with two extracellular matrix (ECM) components viz. fibronectin (FN) and laminin (LN). We found a strong and specific correlation between the lower lateral mobility of phosphatidylcholine (PC) and higher lateral mobility of phosphatidylethanolamine (PE) when cells were expressing high levels of $\alpha5\beta1$ integrin and thus were adherent and motile on FN. The interaction between PC and FN in $\alpha5$ integrin expressing cells was aided by the strong affinity of $\alpha5$ integrin to the FN matrix. Cholesterol was involved in regulating the lateral mobility of PC to a great extent and of PE to a lesser extent without affecting the overall microviscosity of the plasma membrane or the distribution of caveolin-marked domains. The distribution and mobility of PC and PE molecules in the lamellipodial regions differed from that in the rest of the membrane and also in the more motile and in the less motile cells. We propose that these differences in distribution of PC and PE in different regions of cell membrane and their respective lateral mobility are observed due to the specific interaction of PC molecules with FN molecules in the ECM. Our results outline a new role of integrin–matrix interactions in the regulation of membrane phospholipid behavior.

J. Cell. Physiol. 215: 550–561, 2008. © 2007 Wiley-Liss, Inc.

The fluid mosaic model of plasma membrane structure (Singer and Nicolson, 1972; Jacobson et al., 1995) depicts the dynamic constitution and distribution of lipid and protein molecules in the membrane bilayer, determined by factors including cell type, cell physiology, and cytoskeletal architecture. As shown for plasma membranes in vertebrate cells and in model membrane systems, specific proteins and lipids can be transiently confined in nanometer-scaled aggregates, called "domains," causing lateral heterogeneities in the constitution of the plasma membrane (Edidin, 2003; Kraft et al., 2006). One often referred to domain is the "membrane raft," rich in cholesterol (Chol), sphingolipids, and glycosylphosphatidylinositol (GPI) anchored proteins (Simons and Toomre, 2000). However, the existence of raft domains has been controversial due to contradictory biochemical evidence (Munro, 2003). Currently, though these domains are believed to exist in biological membranes, their biochemical constitution is unclear (Groves, 2006). A better-established example of heterogeneity in eukaryotic cell membranes is the asymmetric distribution of various membrane constituents across the transverse plane of the plasma membrane, that is, between the endoplasmic and exoplasmic leaflets of the lipid bilayer (Zachowski, 1993). For example, aminophospholipids, including phosphatidylethanolamine (PE) and phosphatidylserine (PS), reside predominantly in the endoplasmic leaflet, whereas choline-containing phospholipids, including phosphatidylcholine (PC) and sphingomyelin, are localized mainly in the exoplasmic leaflet. Apart from the asymmetrical distribution in the membrane, PC has been reported to be involved in cell signaling (Exton, 1994), and PE in cytokinesis during contractile ring disassembly (Emoto and Umeda, 2000). The structural organization, lateral mobility, and asymmetric distribution of phospholipids and proteins in sperm plasma membranes (Ladha et al., 1997) and rat myocyte

membranes (Yechiel et al., 1985) have been reported. The diffusion coefficients of putative raft- and non-raft-associated proteins in plasma membranes have also been described (Kenworthy et al., 2004). These reports indicate that there are extensive structural and functional heterogeneities in the lipid and protein components of the plasma membrane, but the factors regulating these organizational and functional heterogeneities in intact cells are not well understood.

The influence of extracellular matrix (ECM) components on the organization of lipid molecules in intact cells has not been well analyzed. The few reports that have discussed the role of substrata on the membrane addressed the lateral mobility of PC in endothelial cell membranes (Nakache et al., 1985) and the restricted mobility of lipids and proteins at cell-substrate focal contacts (Geiger et al., 1982; Gaus et al., 2006). The roles of

fibroblast growth factor and ECM on the mobility of a lipophilic fluorescent probe, 5N-[hexadecanoyl]-aminofluorescein (HEDAF), in the basal and apical plasma membranes of endothelial cells have also been described (Tournier et al., 1989). Chol is another major lipid component of the plasma membrane. It intercalates between the fatty acyl chains of the lipid bilayer and is involved in regulating cell adhesion and motility on fibronectin (FN) through integrins (Pande, 2000; Ramprasad et al., 2007). Chol modulates plasma membrane microviscosity in the lamellipodia of moving endothelial cells (Vasanji et al., 2004). Additionally, Chol-dependent distribution of PI(4,5)P2 and actin polymerization in human fibroblasts have been reported (Kwik et al., 2003).

Based on these observations, we hypothesize that adhesion and motility of cells on ECM proteins influence the organization of lipids in the plasma membrane. FN has been shown to self-assemble into fibrillar networks, specifically under a layer of dipalmitoylphosphatidylcholine (DPPC) liposomes (Baneyx and Vogel, 1999). FN conformational changes occur when it is adsorbed onto PC liposomes (Halter et al., 2005). Thus, PC and FN molecules interact directly. Our hypothesis is indirectly supported by findings from a study of the adhesion and proliferation of NIH 3T3 fibroblasts on polylactic acid (PLA) films coated on dioleoylphosphatidylethanolamine (DOPE) vesicles (Fukuhira et al., 2006) and of the diffusion of lipids, including NBD-C_6-PC, NBD-C_6-PE, 5-(N-octa-decanoyl) aminofluorescein (ODAF) and Dil-C_{12}, in various regions of the sperm plasma membrane (Christova et al., 2004). Despite these reports, very little is understood about how the spatial organization and lateral mobility of PC and PE molecules in intact cells is affected by adherence and motility of cells on specific matrix proteins. The involvement of membrane Chol in this process is also unclear. Vasanji et al. (2004) have studied lamellipodial plasma membrane microviscosity, but they have not reported the dynamics and reorganization of PC and PE molecules in the lamellipodial regions of cells that are in close contact with matrix proteins.

Therefore, we analyzed how two ECM proteins, FN and laminin (LN), influence the lateral mobility of PC and PE in intact cells that are highly motile on these two substrata. We used L27 cells as a prototype for this study; the properties of these cells have been reported previously (Beauvais et al., 1995; Ramprasad et al., 2007). We used D711 cells as a control cell type to show the specificity of our results. These cells are derived from the same parental cells as L27, but overexpress $\alpha 4\beta 1$ integrin and exhibit less spreading and motility on FN. We carried out the same analysis after depletion of Chol from the membrane with methyl-beta-cyclodextrin (MBCD) and its replenishment with Chol-loaded MBCD (CHO-MBCD). We found strong substratum and integrin-specific influences on the lateral mobility of PC and PE molecules in the plasma membrane, and on actin organization in the cytoplasm. These influences were stronger in the lamellipodial regions of the membrane, indicating that PC and PE molecules are involved in the formation and extension of lamellipodia during cell motility.

Materials and Methods
Reagents

MBCD, LN from human placenta, Thiazolyl Blue Tetrazolium Bromide (MTT) reagent for cell viability assay and non-enzymatic cell dissociation solution were obtained from Sigma (St. Louis, MO). Chol-loaded MBCD (CHO-MBCD) complex was obtained from Cyclodextrin Technologies Development Inc. (High Springs, FL). Lab-Tek II chambered cover glass was obtained from Nalge Nunc International (Naperville, IL). NBD-C_6-PC (2-(6-(7-nitrobenz-2-oxa-1,3-diazol-4-yl)amino)-hexanoyl-1-hexadecanoyl-sn-glycero-3-phosphocholine), NBD-PE (N-(7-nitrobenz-2-oxa-1,3-diazol-4-yl)-1,2-dihexadecanoyl-sn-glycero-

3-phosphoethanolamine, triethylammonium salt), DPH (1,6-diphenyl-1,3,5-hexatriene), rhodamine DHPE (Lissamine™ rhodamine B 1,2-dihexadecanoyl-sn-glycero-3-phosphoethanolamine, triethylammonium salt) and rhodamine-phalloidin were obtained from Molecular Probes (Invitrogen, Eugene, OR). Anti-caveolin polyclonal antibody was obtained from Transduction Laboratories (Lexington, KY). BM Chemiluminescence Western blotting kit was purchased from Roche Molecular Biochemicals (Mannheim, Germany). Human cellular FN was purchased from Upstate Cell Signaling Solutions (Lake Placid, NY). Two hexameric peptides—GRGDSP and GRGESP—were synthesized and purified at the peptide synthesis facility at CCMB.

Cell cultures and membrane-chol depletion and restoration

The cells were cultured in DMEM (Sigma), supplemented with 10% FCS (Sigma and Invitrogen), streptomycin (50 μg/ml), and penicillin (60 μg/ml). The cells were grown in an atmosphere of 5% CO_2 at 37°C. For depletion of Chol from the plasma membrane, cells were serum-starved for 2 h in DMEM and then treated with 10 mM MBCD in serum-free DMEM for 30 min. For restoration of Chol levels in the membrane, the MBCD-containing DMEM was removed; the cells were washed with serum-free DMEM and then treated with CHO-MBCD in serum-free DMEM (final concentration 100 μM Chol component) for 2–4 h.

Coating of substratum and preparation of cells

Tissue culture dishes, chambered cover glasses or cover slips were coated with either 5 μg/ml FN or 30 μg/ml LN prepared in PBS and incubated at 4°C overnight, as described previously (Dufour et al., 1999). Cells growing exponentially were dissociated using non-enzymatic cell dissociation solution and 1.5×10^5 cells were seeded on the coated cover glasses or cover slips. The cells were allowed to adhere and spread for 2 h in serum-free DMEM. Spread cells were prepared for cholesterol depletion/restoration and fluorochrome labeling.

Labeling of cells for fluorescence recovery after photobleaching (FRAP) or fluorescence imaging

Untreated cells, MBCD-treated cells or CHO-MBCD-treated cells plated on FN-coated, LN-coated or uncoated cover slips were washed with HEPES-buffered Hanks balanced salt solution (HBSS) to remove the DMEM. For FRAP, the cells were then labeled with the ethanolic solution of NBD-PC (6.5 μM) or NBD-PE (30–60 μM) in the same buffer at room temperature (25–27°C) for 5–10 min. For dual labeling used in imaging, cells were first labeled with approximately 9 μM of ethanolic solution of rhodamine-PE in HBSS for 5 min at room temperature, rinsed with HBSS once and then labeled with 6.5 μM NBD-PC in HBSS for 5 min at room temperature. The cells were rinsed twice with HBSS and analyzed by FRAP or fluorescence imaging.

FRAP analysis

Lateral mobility of the NBD-PC or NBD-PE dyes was measured by FRAP analysis of cells labeled with a single dye. FRAP experiments were done at 25°C with a Zeiss LSM 510 Meta confocal microscope.

Initially, FRAP analysis was done for a well-labeled, non-lamellipodial region of the cell membrane, with a 40X objective of NA 0.85 focused at a plane of 0.5–0.8 μm thickness just above the basal surface of the cell, which was in contact with the substratum—this was to ensure that fluorescence only from the basal membrane was considered for FRAP. A 30 mW laser beam at a wavelength of 488 nm with Gaussian cross-sectional intensity was used for spot bleaching. An attenuated laser beam over a period of 120 sec with an interval of 0.58 sec between each postbleach scan was used to monitor fluorescence recovery. Subsequently, FRAP analysis was done for lamellipodial regions with a 63X/1.2 NA

water immersion objective. For such analysis, a spot scan with a radius of 1.4 μm was chosen within the lamellipodial region. In order to ensure that the fluorescence only from the basal membrane is considered, the thickness of the focal plane of the objective was kept at 0.2–0.4 μm above the basal surface of the cell. Wherever it could not be ensured that the fluorescence was exclusively derived from the basal surface of the cells, those lamellipodia were not considered for analysis. From this point on, the protocol was the same as that used for measurements in the non-lamellipodial region. The physical parameters of FRAP recovery in both lamellipodial and non-lamellipodial regions were analyzed by doing the best curve fit of the mean membrane versus cytoplasm fluorescence intensities obtained in the region of interest (ROI) before and after the bleach. The method of Yguerabide et al. (1982) was used for determining values for the half-time of the recovery ($t_{1/2}$) and the diffusion constant (τ_d). The value of the beam radius (ω) was estimated according to the standard operating procedure for microscope software (LSM-FCS). These values were used in each experiment to calculate the value for lateral diffusion or mobility (D) of the fluorescent molecule. Such D values of NBD-PC and NBD-PE were calculated under various conditions for each cell type. At least 10–15 cells were studied in each experiment for the determination of the mean D value. We compared mean D values of NBD-PC and NBD-PE in various cell types and under various conditions. The Student's t-test was used to determine the significance of the differences in D values.

FRAP analysis after treatment of cells with bioactive peptides

5×10^5 L27 cells, suspended in DMEM without serum, were treated with varying concentrations (8–48 μM) of GRGDSP and GRGESP (24 μM) for 1 h at 37°C and plated on chambered cover glass coated with 5 μg/ml FN. After the cells had attached and spread on FN, they were labeled with NBD-PC and FRAP analysis of PC mobility was done as described above. The results were analyzed in comparison to treated versus untreated control cells.

Dual fluorescence imaging and time-lapse imaging by confocal microscopy

Untreated L27 cells plated on FN- or LN-coated chambered coverglasses were labeled with NBD-PC and Rhodamine-DHPE at room temperature as described above. Images of the cells labeled for dual fluorescence were acquired at 25°C with an inverted Zeiss LSM 510 META confocal microscope with a 63X/1.2 NA water-immersion objective with the 488 nm line of an argon ion laser for NBD-PC and 543 nm line of a He-Ne laser for rhodamine-PE. For time-lapse imaging, rhodamine-PE and NBD-PC labeled cells plated on FN- or LN-coated 40 mm cover slips were transferred to a Bioptechs FCS2 closed chamber filled with phenol red-free DMEM and maintained at 37°C. The FCS2 system was fitted on a Zeiss LSM 510 META confocal microscope. Images of cells labeled for dual fluorescence were acquired at 37°C, in intervals of 30 sec for 20 min.

DPH fluorescence polarization and anisotropy

We measured membrane fluidity of L27 cells plated on plastic, FN or LN by estimating fluorescence polarization of 1,6 diphenyl-1,3, 5- hexatriene (DPH), as described previously (Gopalakrishna et al., 2000). Cells, while still attached to their substrata, were incubated at 37°C with 1 μM DPH in DMEM for 20 min. Unincorporated dye was removed by repeated washings with DMEM. Labeled cells were suspended at a concentration of 0.6–0.8×10^6 cells/ml in PBS. We measured polarization values at various cell concentrations, as described previously (Lentz et al., 1979), to take light scattering into account. We used a Hitachi F-4000 spectrofluorimeter equipped with a polarizer attachment to measure fluorescence of incorporated dye at 358 nm [λ_{ex}] and 430 nm [λ_{em}] in cells constantly stirring at room temperature. Fluorescence polarization

values were calculated using the equation:

$$P = [I_{VV} - GI_{VH}]/[I_{VV} + GI_{VH}].$$

Fluorescence anisotropy values were calculated using the equation:

$$R = [I_{VV} - GI_{VH}]/[I_{VV} + 2GI_{VH}],$$

where I_{VV} and I_{VH} are fluorescence intensities observed with the emitted light polarizer in vertical or horizontal position, respectively, with respect to the excitation polarizer. G is the grating correction factor.

Caveolin distribution in membranes

Approximately 6×10^6 L27 cells were grown on plastic or plated on FN- or LN-coated 10 cm dishes. Chol depletion and restoration were done as described above. Lysates of each cell type were prepared on ice in 1 ml of lysis buffer containing 50 mM Tris–HCl (pH 7.4), 150 mM NaCl, 2 mM NaF, 1 mM EDTA, 1 mM EGTA, 1 mM NaVO$_3$.H$_2$O supplemented with 20 μg/ml each of aprotinin and leupeptin, 1 mM PMSF, and 0.5% Brij 96. The lysates were kept on ice for 30 min, sonicated with a Branson sonicator, passed through a 28G needle five times and centrifuged. The protein content of the supernatant was measured with a BioRad protein assay mixture. Caveolin distribution was assessed by sucrose density gradient fractionation of the lysates. The bottom of a 4.2 ml Beckman polyallomer centrifuge tube was filled with a mixture of 0.9 ml of each type of cell lysate and 0.9 ml of 90% sucrose, making 1.8 ml of 45% sucrose solution. The 45% sucrose layer was overlaid with 1.2 ml of 35% sucrose in lysis buffer, which was overlaid with 1 ml of 5% sucrose in lysis buffer. Each step was done at 4°C. The sucrose density gradients were placed in a SW60Ti rotor and centrifuged at 45,000 rpm in a Beckman ultracentrifuge for 21 h at 4°C. Afterwards, ten 400-μl fractions from each tube were collected and kept on ice.

We determined the distribution of caveolin in these gradient fractions. An equal volume of each fraction was boiled in 3X SDS sample buffer with 2-mercaptoethanol and analyzed by 10% SDS–PAGE. Caveolin was detected by western blot analysis with anti-caveolin antibody followed by anti-rabbit IgG-POD labeled secondary antibody and visualized with the BM chemiluminescent substrate.

F-actin staining and imaging

F-actin was stained with rhodamine-phalloidin as described previously (Gopalakrishna et al., 2004). Images were visualized using a Plan Apochromat 100X/NA1.4, oil-immersion DIC objective in a Zeiss Axio Imager.Z1 microscope with ApoTome® module, using the Zeiss Axiovison software. The corresponding differential interference contrast (DIC) images of rhodamine-phalloidin stained cells were taken with the same objective.

Results
Lateral mobility of PC under various conditions

Lipids that are covalently labeled with a NBD group are widely used as fluorescent analogues of native lipids in biological membranes to study a variety of membrane related processes (Chattopadhyay, 1990). We wanted to assess the role of ECM proteins, FN or LN, and various integrins in modulating the lateral mobility of phospholipids in intact cells. We studied the lateral mobility of the NBD-tagged PC (a predominant lipid in the outer leaflet of the bilayer) or PE (a predominant lipid in the inner leaflet of the bilayer) (Zachowski, 1993) by doing FRAP analysis of S180, L27, and D711 cells labeled with these dyes and plated on various substrata. L27 and D711 are stably transfected clones derived from the parental mouse sarcoma

S180 cell line, as described previously (Beauvais et al., 1995; Ramprasad et al., 2007). L27 clones express about fivefolds higher levels of FN-specific high affinity $\alpha5\beta1$ integrins in comparison to S180 parental cells. D711 cells express high levels of low affinity FN-specific $\alpha4$ integrins but low levels of $\alpha5\beta1$ integrin. Therefore L27 cells adhere and move faster than D711 cells on FN but they behave similarly on LN and experiments with L27 cells have been used to specifically evaluate the $\alpha5\beta1$ mediated cell functions.

A representative FRAP experiment with NBD-PC-labeled L27 cells plated on LN is described in Figure 1A,B. We chose a well-labeled region (ROI-1) of the plasma membrane in the non-lamellipodial area of the cell for FRAP analysis. We used an adjacent, poorly labeled region (ROI-2) in the cytoplasm of the same cell to determine the specificity of the bleach in ROI-1.

The fluorescence in ROI-1 was more than 60% bleached and then recovered by more than 50%. There was no significant change in fluorescence in ROI-2. Recovery curves for ROI 1 and ROI 2 (Fig. 1B) show that ROI 1 had the typical FRAP recovery pattern, whereas fluorescence levels in ROI 2 changed insignificantly during the experiment. We took similar measurements in 10–15 cells for each cell type in each experiment and averaged the values from each experiment to calculate the overall lateral mobility of NBD-PC molecules. For each cell type and condition, the experiment was repeated at least three times.

We compared the average NBD-PC mobility values from S180, L27 and D711 cells plated on FN, LN, and plastic (PL) (Fig. 1C). In general, NBD-PC mobility on FN was very low in all three cell types, but L27 cells had the lowest NBD-PC mobility on FN (2.22×10^{-10} cm^2/sec) (Fig. 1C). However, NBD-PC mobility was 4.5 times higher in L27 cells plated on LN than on FN ($P < 0.05$). NBD-PC mobility in S180 cells plated on FN and LN was similar and NBD-PC mobility was 2.07 times higher in D711 cells plated on LN than FN ($P = 0.05433$). NBD-PC mobility in these three cell types plated on LN was not significantly different. NBD-PC mobility was very low in all three cell types if they were plated on PL, a non-specific substratum.

These results indicate that when cells interact with specific ECM substrata, there is differential and higher lateral mobility of NBD-PC molecules than when these cells are plated on PL. The lateral mobility of NBD-PC was much lower in L27 cells strongly attached to FN, due to high expression levels of FN-specific $\alpha5$ integrin, than in L27 cells plated on LN. The $\alpha5$ integrin is not a receptor for LN, and the cells adhere to LN through other integrins they express at moderate levels such as $\alpha3\beta1$ and $\alpha6\beta1$ (Ramprasad et al., 2007). On FN, NBD-PC mobility was slightly higher in D711 cells than in L27 cells. D711 cells express high levels of FN-specific $\alpha4$ integrin, but are less adherent to FN than L27 cells (Ramprasad et al., 2007). In D711 cells, though NBD-PC mobility was higher if they were plated on LN than on FN, the difference was smaller than what we observed for L27 cells. We observed similar NBD-PC mobility for L27 and D711 cells plated on LN, also indicating substrate selectivity.

The percentage of the mobile fraction of the total NBD-PC molecules during the FRAP process under various conditions (Table 1A) support these findings. The percentage of the mobile fraction of NBD-PC in L27 cells correlates well with the overall average mobility of NBD-PC molecules. Typically, $46.55 \pm 15.5\%$ of NBD-PC molecules were mobile on FN, $77 \pm 9.54\%$ were mobile on LN. This implies that most of the NBD-PC molecules associated with FN, whereas much fewer NBD-PC molecules associated with LN. Similarly, D711 cells also showed a lower percentage of mobile NBD-PC molecules on FN and a higher percentage of mobile NBD-PC molecules on LN, corresponding to the relative interaction of the $\alpha4$ integrin with FN and LN (Table 1A).

In order to determine the direct involvement of $\alpha5\beta1$ integrin in regulation of lateral mobility of PC molecules, we treated L27 cells with the RGD bearing specific peptide ligand of the $\alpha5\beta1$ integrin (GRGDSP) and its non-active counterpart GRGESP as described in Materials and Methods Section. We observed that cells treated with RGD containing peptides did not spread well on the FN coated substratum (Fig. 2A) whereas untreated or RGE peptide treated cells were well spread. This indicated that the RGD peptide treatment had inhibited the biological activity of the integrin. Under these conditions, the analysis of NBD-PC lateral mobility showed that when cells were treated with RGD peptides, NBD-PC mobility increased by two to fourfolds depending upon the concentration of the peptide used (see Fig. 2B). Such a change in PC mobility was not observed when the cells were treated with RGE peptide. The fluorescence recovery curves shown in Figure 2C also indicate a similar change in the pattern of PC mobility after peptide treatment.

Lateral mobility of NBD-PE under various conditions

The patterns for lateral mobility of NBD-PE in these three cell types plated on FN and LN were different than what we observed for NBD-PC mobility. However, NBD-PE mobility and NBD-PC mobility were similar in these cells plated on PL (Fig. 1D). In general, NBD-PE mobility was higher than that of NBD-PC for all three cell types tested if they were plated on FN, but mobility of NBD-PE was especially high (2.5×10^{-9} cm^2/sec) in L27 cells plated on FN. Though, NBD-PE mobility in cells plated on LN was significantly lower than in cells plated on FN for all three cell types, the difference was more significant for S180 (5.05 times lower) and L27 cells (4.02 times lower) than for D711 cells. Thus, though both NBD-PC and NBD-PE had higher lateral mobility when the cells were in contact with specific ECM substrata, NBD-PE molecules moved much faster than NBD-PC molecules in L27 cells plated on FN.

Values for mobile fractions of PE molecules in these three cell types on FN and LN were similar (Table 1B). Seventy percent of NBD-PE molecules in L27 cells on FN and approximately 80% on LN were mobile. This suggests that NBD-PE molecules were not strongly associated with either FN or LN. S180 and D711 cells on FN and LN also had considerable amounts of highly mobile NBD-PE. If grown on PL, the overall mobility of NBD-PE molecules in L27 and D711 cells was low, but was considerably higher in S180 cells. The recovery curves for NDB-PC and NBD-PE for L27 cells on the three types of substrata tested showed high recovery for NBD-PE on FN and NBD-PC on LN (Fig. 1E).

Membrane chol and lateral mobility of NBD-PC and NBD-PE

We examined the lateral mobility of NBD-PC and NBD-PE after depletion and restoration of membrane Chol in cells plated on FN and LN. Cell viability under both these conditions was >90% (data not shown). After cholesterol depletion, NBD-PC mobility was 12.5 times higher in L27 cells on FN than in untreated cells. On LN, NBD-PC mobility was 2.2 times lower than in untreated cells. NBD-PC molecules were significantly less mobile in cells on FN following Chol restoration, with levels of mobility nearly that observed in untreated cells. In cells on LN, the level of NBD-PC mobility reached the same level as that seen in untreated cells (Fig. 3A). In D711 cells plated on FN, NBD-PC mobility was 4.5 times higher after Chol depletion and reached untreated levels if Chol was restored (Fig. 3A). In D711 cells plated on LN, Chol depletion and restoration did not significantly change NBD-PC mobility (Fig. 3A). Additionally, Chol depletion did not significantly change NBD-PC mobility in S180 cells plated on FN and LN (Fig. 3A).
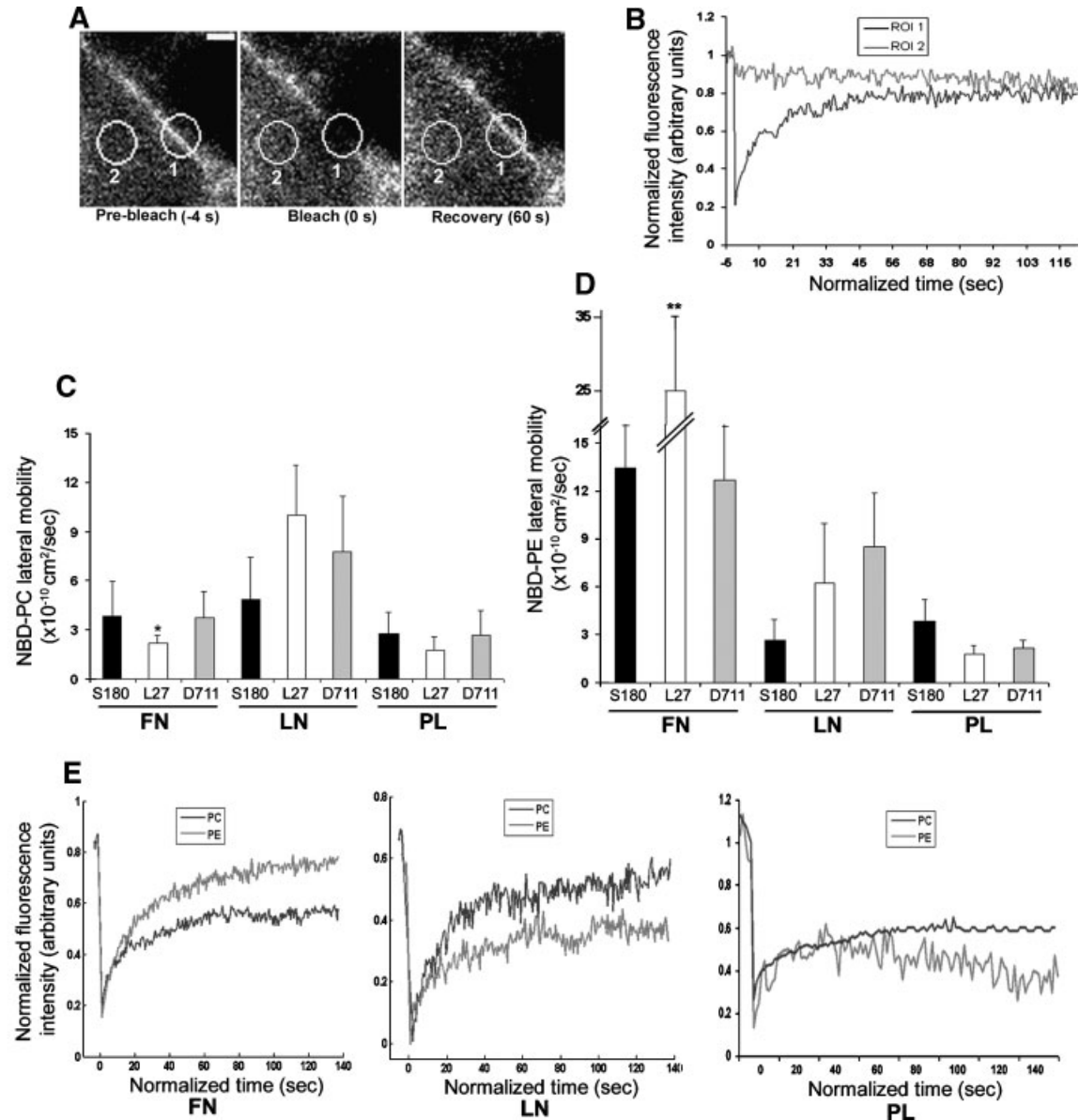
Fig. 1.   Lateral mobilities of NBD-PC and NBD-PE on various substrata and in cells expressing different integrins. A: A representative FRAP experiment in the non-lamellipodial region of a L27 cell plated on LN and labeled with NBD-PC. We magnified a cell with sharp labeling of NBD-PC by a factor of 2 and chose a square region for FRAP analysis. Circular region of interest 1 (ROI 1), with a radius of 1.4 μm, on the membrane was chosen for FRAP and the adjacent ROI 2, (2 μm apart from ROI 1) near the membrane, inside the cell, served as an internal control to show the specificity of bleach in ROI 1. The left part shows the pre-bleach scan, 4 sec before bleach. The middle part shows the image just after the bleach; fluorescence intensity diminishes only in membranous ROI 1, but not in ROI 2. The right part shows the recovery of fluorescence in ROI 1, 60 sec after bleach. Bar, 2 μm. B: Fluorescence intensity of NBD-PC in the membranous region of ROI 1 (black curve) and in the cytoplasmic region of ROI 2 (gray curve) over time during the FRAP experiment in A. ROI 1 in the membrane shows a decrease of about 77% in the fluorescence intensity after bleach followed by a significant recovery. There is no significant change in the fluorescence intensity in ROI 2 in the cytoplasm near the membrane, showing the specificity of the bleach region in ROI 1. C: Mean lateral mobility of NBD-PC in the non-lamellipodial regions of untreated S180, L27, and D711 cells plated on FN, LN, or PL. *Indicates that PC mobility in L27 cells plated on FN is significantly lower ($P \leq 0.05$) than that in S180 or D711 cells on FN. D: Mean lateral mobility of NBD-PE in the non-lamellipodial regions of untreated S180, L27 and D711 cells plated on FN, LN or PL. **Indicates that PE mobility in L27 cells plated on FN is significantly higher ($P \leq 0.05$) than that in S180 or D711 cells on FN. E: Representative FRAP recovery curves for NBD-PC (black) and NBD-PE (gray) molecules in the non-lamellipodial regions of L27 cells plated on FN, LN, or PL.

There were no significant changes in the mobility of NBD-PE molecules after cholesterol depletion and restoration in L27, D711 and S180 cells plated on FN and LN (Fig. 3B). Therefore, membrane cholesterol predominantly affected the lateral mobility of PC molecules in α5 and α4 integrin expressing cells on FN.

ECM-related caveolin redistribution in the membrane

Caveolin is predominantly found in caveolae, which are 100 nm invaginations of Chol-enriched membrane microdomains. Caveolins bind Chol and as the structure of caveolae is dependent on Chol, caveolae disappear after Chol removal

TABLE 1. Percent recovery or percent mobile populations of (A) NBD-PC and (B) NBD-PE following FRAP experiments in untreated S180, L27, and D711 cells plated on FN, LN, or PL

	Cell type		
Substratum	S180	L27	D711
(A) PC			
FN	49 ± 13.9	46.55 ± 15.5	50.5 ± 20.7
LN	65.25 ± 22.29	77 ± 9.54	63.16 ± 14.6
PL	49.6 ± 13.05	55.3 ± 11.17	44.13 ± 15.43
(B) PE			
FN	60.6 ± 15.79	69.85 ± 18.37	55.16 ± 3.3
LN	65.83 ± 18.04	79.5 ± 13.7	72.5 ± 21.3
PL	63.85 ± 15.86	55 ± 21.35	52.25 ± 19.75

(Razani et al., 2002). Phosphorylation of caveolin at Tyr14 is involved in internalization of Chol-enriched membrane microdomains in an integrin-dependent manner (del Pozo et al., 2005). Caveolae are a subset of lipid rafts and caveolin is used as a marker protein to identify detergent-resistant membranes (Parton et al., 2006). Thus, we tested L27 cell lysate density gradient fractions for the presence of caveolin to study the distribution of caveolar domains in these cells plated on various substrata.

We detected caveolin in all the high- and low-density fractions of the sucrose density gradient for L27 cells plated on FN. Caveolin distribution did not change much after Chol depletion, except that it was not present in one of the lighter (upper most) fractions. Caveolin distribution following Chol restoration was similar to that seen in untreated cells (Fig. 3C).

Caveolin distribution in L27 cells plated on LN was distinctly different from that in these cells plated on FN: caveolin distribution was mostly restricted to mid-density fractions 4, 5, 6, and 7. Chol depletion did not affect this distribution. Following Chol restoration, caveolin was present above the interface of 5% and 35% sucrose, in fraction 3, in addition to the middle fractions (Fig. 3D).

Caveolin was present in all the density gradient fractions, except the lightest fraction, in L27 cells plated on the non-specific substratum PL. Though Chol depletion mostly restricted caveolin to the higher density fractions, caveolin was also present in the lighter density fraction 2. Following Chol restoration, caveolin distribution was restricted to fractions in mid-density, 35% sucrose and two fractions in high-density, 45% sucrose (Fig. 3E).

Thus, Chol removal and restoration in L27 cells plated on FN, LN or PL did not significantly alter the distribution of caveolin-rich membrane domains, but significantly affected the lateral mobility of NBD-PC molecules in these cells plated on FN.
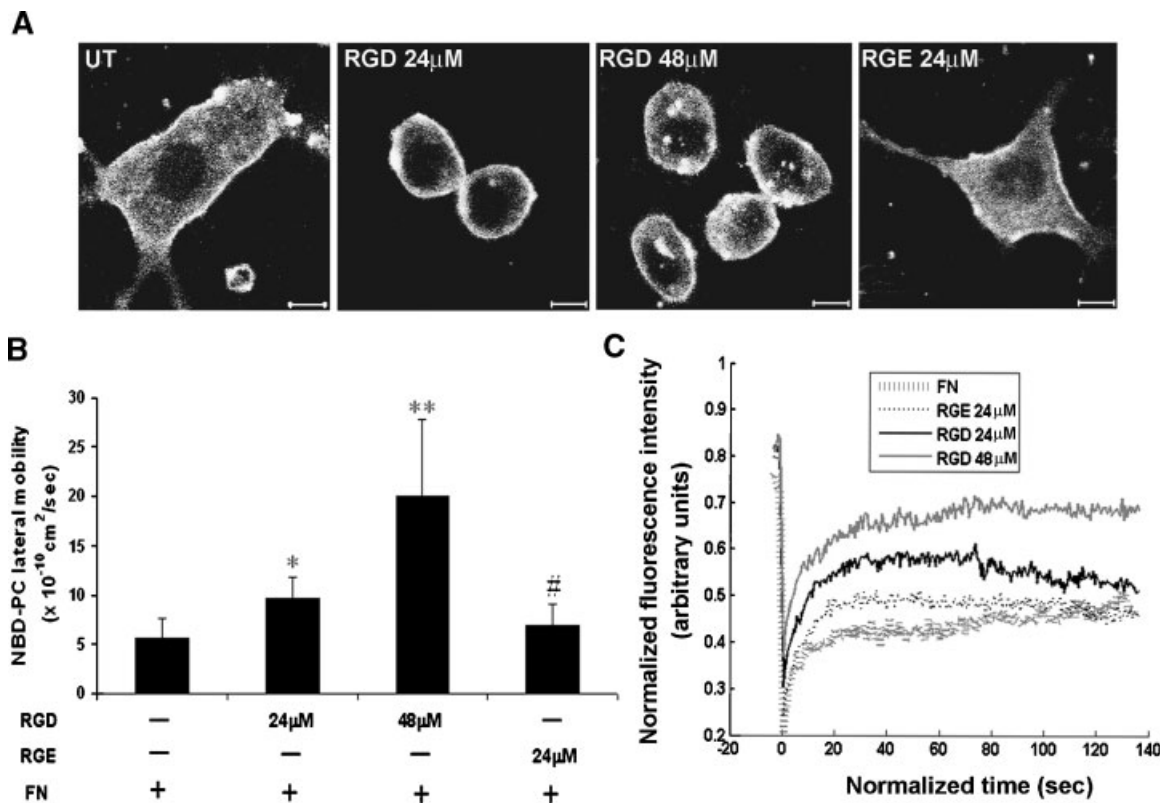

Fig. 2. Effect of integrin specific bioactive peptides on the morphology of L27 cells plated on FN and on the lateral mobility of NBD-PC in L27 cells plated on FN. Part (A) represents the morphology of either untreated (UT) L27 cells or L27 cells pre-treated with the indicated concentrations of RGD, RGE peptides, plated on FN and labeled with NBD-PC. Bars, 10 μm. Part (B) represents the average lateral mobility of NBD-PC molecules in 15–18 L27 cells plated on FN without any treatment or with the pre-treatment of RGD (24 μM), RGD (48 μM), RGE (24 μM). The NBD-PC labeled membranes in the non-lamellipodial regions were chosen for the FRAP analysis. *Represents a significant increase ($P < 0.05$) in the lateral mobility of NBD-PC in RGD (24 μM) treated cells in comparison to untreated cells. **Represents a significant increase ($P < 0.001$) in the lateral mobility of NBD-PC in RGD (48 μM) treated cells in comparison to untreated cells. #Represents an insignificant change in the average lateral mobility of NBD-PC in RGE treated cells in comparison to untreated cells. Part (C) represents the fluorescence recovery curves after photobleaching of NBD-PC molecules in L27 cells plated on FN without any treatment or with pre-treatment of indicated peptides in part B.
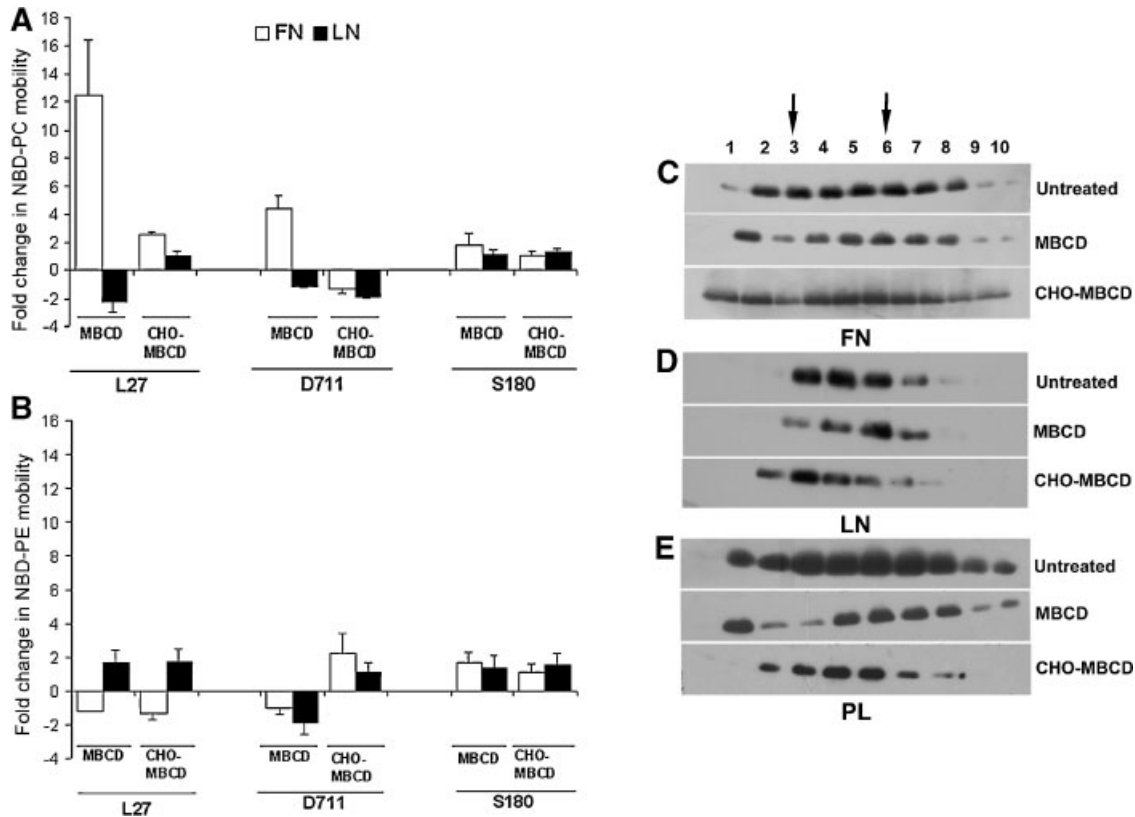
Fig. 3. Changes in lateral mobility in L27, D711, and S180 cells after Chol modulation and caveolin distribution in L27 cells on different substrata. **A:** Fold change in NBD-PC mobility in L27, D711, and S180 cells plated on FN (white bars) or LN (black bars) after treatment with MBCD and CHO-MBCD. Values indicate the change in mobility with respect to the corresponding untreated cells. **B:** Fold change in NBD-PE mobility in L27, D711, and S180 cells plated on FN (white bars) or LN (black bars) after treatment with MBCD and CHO-MBCD. Values indicate the change in mobility with respect to corresponding untreated cells. **C–E:** Sucrose density gradient analysis for the distribution of caveolin-1 molecules in L27 cells plated on (C) FN, (D) LN, and (E) PL without treatment, after 30–40 min of MBCD treatment and after 2 h of Chol restoration (CHO-MBCD). Fraction 1 is of lightest density and fraction 10 is of highest density. The arrow at fraction 3 indicates the position of the interface between 5% and 35% sucrose in the gradient. The arrow at fraction 6 indicates the position of the interface between 35% and 45% sucrose in the gradient.

Distribution of NBD-PC and rhodamine-PE in lamellipodial regions

L27 cells when plated on different ECM proteins formed different membrane protrusions—large lamellipodia on FN and long filopodia and smaller lamellipodia on LN (Ramprasad et al., 2007). Hence, we wanted to check the role of ECM proteins FN or LN in the distribution of NBD-PC and Rhodamine-PE in L27 cells and in their protrusive structures. We used a confocal microscope to acquire images of live L27 cells within 20 min of rhodamine-PE and NBD-PC labeling, to avoid endocytosis of lipids. NBD-PC and rhodamine-PE clearly and equally colocalized in the membrane in most parts of L27 cells plated on FN, but not in the lamellipodium (Fig. 4A, upper part). We observed more rhodamine-PE than NBD-PC in the membrane on the leading edge of a forming lamellipodium (Fig. 4A, inset i), the trailing edge of a retracting lamellipodium (Fig. 4A, inset ii) and the interior of the lamellipodium. The colocalization of the two molecules was not continuous along the lamellipodial membrane. We observed rhodamine-PE labeling on the membrane, outside the boundaries of NBD-PC distribution. In these L27 cells plated on FN, we also detected more rhodamine-PE than NBD-PC in the cytoplasm. The fluorescence intensity profile of rhodamine-PE and NBD-PC at

the leading edge of a forming lamellipodium (Fig. 4A, inset i) is shown in Figure 4C.

Our findings for L27 cells plated on LN were different than for those plated on FN. Fewer lamellipodia formed in cells plated on LN than on FN. These were thinner, longer and more filopodia-like than the broad and flat lamellipodia that formed in cells on FN. The intensity of NBD-PC labeling was stronger than that of rhodamine-PE labeling in these long membrane extensions. The colocalization pattern was similar throughout the cell (Fig. 4A, lower part). Enlarged portions of the lamellipodia are shown in Figure 4A, insets (iii) and (iv). The fluorescence intensity profile for NBD-PC and rhodamine-PE distribution in Figure 4A inset (iii) is shown in Figure 4D. Whereas L27 cells on FN make large lamellipodia (~7 μm), on LN they make small lamellipodia (~3 μm). The approximate width of the lamellipodia is evident from the profiles of fluorescence intensities for NBD-PC and rhodamine-PE distribution (Fig. 4C,D).

DIC images (Fig. 4B) show that L27 cells formed more lamellipodia on FN and more filopodial structures on LN. F-actin had a meshwork-like distribution at the leading edge of lamellipodia in L27 on FN. On LN, bundles of parallel-arranged F-actin filaments protrude from the tip of the filopodial structures. These findings indicate that rhodamine-PE localizes
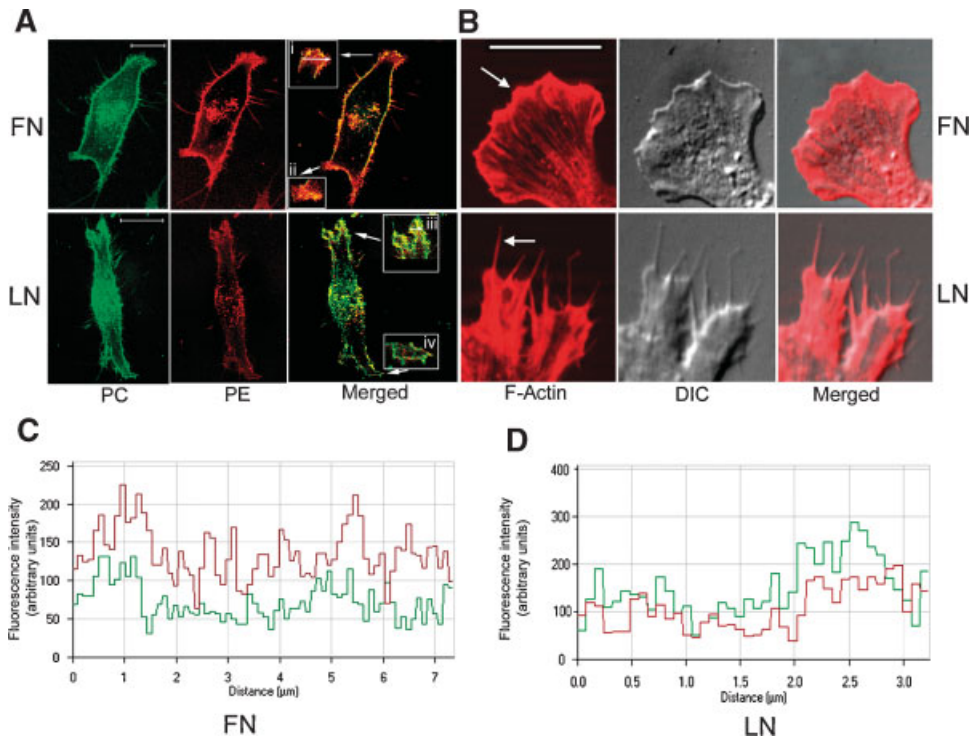
Fig. 4. Distribution of NBD-PC, rhodamine-PE, and F-Actin in L27 cells plated on various substrata. A: Confocal images of L27 cells plated on FN (upper parts) and on LN (lower parts), labeled with NBD-PC (left parts) and rhodamine-PE (middle parts). Merged images show colocalization of NBD-PC and rhodamine-PE (right parts). Insets i and ii on FN show the distribution of NBD-PC and rhodamine-PE at the leading edge of a broad lamellipodium and at the trailing edge of a cell, respectively. Insets iii and iv on LN show the distribution of NBD-PC and rhodamine-PE in the narrow lamellipodia at the leading edge and at the trailing edge of a cell respectively. Scale bars represent 10 μm. B: Meshwork-like F-actin distribution (upper left part) in the leading edge of a lamellipodium (indicated by arrow) of a L27 cell plated on FN. The corresponding DIC image (upper middle part) and the merged image (upper right part) are also shown. The lower left part depicts the parallel bundles of F-actin distribution in the filopodia-like structures (indicated by arrow) of L27 cells plated on LN. The corresponding DIC image (lower middle part) and the merged image (lower right part) are also shown. Scale bars represent 10 μm. Fluorescence intensity profile of NBD-PC and rhodamine-PE distribution in the lamellipodial region (marked in A, inset i) of L27 cells on FN (C) and in the smaller lamellipodia and filopodia-like region (marked in A, inset iii) of L27 cells on LN (D). The red peaks represent rhodamine-PE and the green peaks represent NBD-PC.

more in lamellipodia on FN and NBD-PC localizes more on the smaller lamellipodia on LN.

Dynamics of NBD-PC and rhodamine-PE distribution

We used time-lapse imaging to assess the dynamic distribution of NBD-PC and rhodamine-PE in motile L27 cells, in their lamellipodia and filopodia when plated on various substrata.

L27 cells plated on FN formed flat lamellipodia and were more motile than those plated on LN. NBD-PC and rhodamine-PE colocalized in the whole cell, but rhodamine-PE surged ahead of NBD-PC in the leading edge of a forming lamellipodium. There was increased vesicular trafficking of rhodamine-PE toward the leading edge (Supplementary movie 1). The protruding lamellipodium moved approximately 4 μm over a period of 20 min. At the beginning of lamellipodial formation (0 min), NBD-PC and rhodamine-PE were distributed equally in the lamellipodial membranes and their fluorescence intensities were almost the same (Fig. 5A,B). As the lamellipodium expanded, the fluorescence intensity of rhodamine-PE (red) gradually increased, but the fluorescence intensity of NBD-PC (green) gradually decreased. Whereas distribution of NBD-PC was restricted to the membrane of the lamellipodium, rhodamine-PE was present in the membrane and the cytoplasm of the lamellipodium (Fig. 5A). The mean fluorescence intensity of rhodamine-PE gradually increased

over NBD-PC after 12 min of the lamellipodial protrusion (Fig. 5B).

L27 cells plated on LN formed protruding filopodial structures and smaller lamellipodia than these cells plated on FN. We observed NBD-PC and rhodamine-PE colocalization in the plasma membrane of the whole cell, with the exception of the smaller lamellipodium and many filopodia. Over 20 min, the observed cell had very low motility; very little motion occurred even in the small lamellipodium (Supplementary movie 2). There was a very high concentration of NBD-PC and a low concentration of rhodamine-PE in the leading edge and filopodial structures throughout the time course (Fig. 5C). The mean fluorescence intensity of NBD-PC in the small, protruding lamellipodium was higher than rhodamine-PE at all time points tested (Fig. 5D). Thus, ECM proteins played an important role in the differential distribution and dynamics of NBD-PC and rhodamine-PE in the cellular protrusions formed on FN or LN.

Extracellular matrix affects the lateral mobility of NBD-PC and NBD-PE in lamellipodia

As the distribution of lipids in the lamellipodia was different than that in the rest of the cell membrane, we studied the ECM induced dynamic changes in lipid mobility in these structures. We used confocal microscopy to carry out FRAP analysis of lamellipodial regions in L27 cells labeled with NBD-PC or
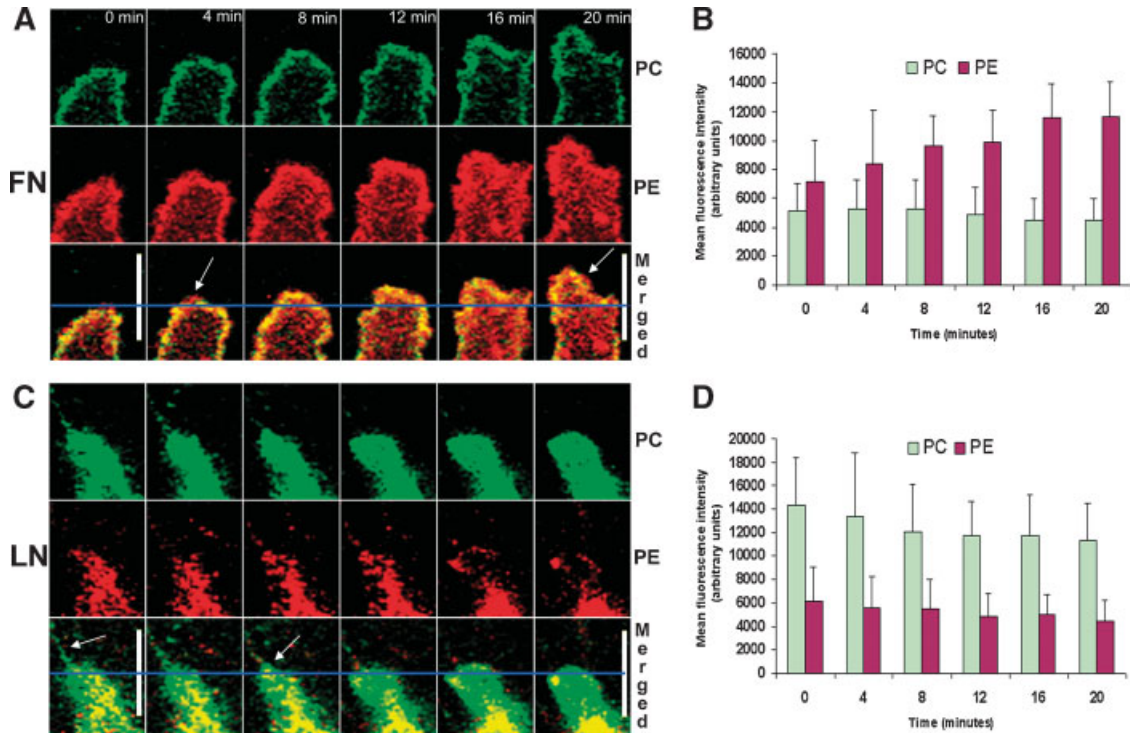
Fig. 5. Dynamics of NBD-PC and rhodamine-PE distribution in L27 cells. A: Frames from Supplementary movie 1 depicting the distribution of NBD-PC (top row), or rhodamine PE (middle row), and merged images (bottom row) in the lamellipodium of a representative L27 cell plated on FN. The frames were taken at intervals of 4 min. The arrows in the merged images indicate the points of surface exposition of rhodamine-PE at the leading edge of the lamellipodium. The horizontal line across the merged images indicates the level from which the lamellipodium starts to protrude. Bar, 10 μm. The approximate distance of the forward movement of the lamellipodium from the basal level is around 4 μm. B: Mean fluorescence intensity of NBD-PC and rhodamine-PE in the merged images at all time points depicted in (A). C: Frames from Supplementary movie 2 depicting the distribution of NBD-PC (top row), rhodamine-PE (middle row), and merged images (bottom row) in the small lamellipodium and the filopodium of a representative L27 cell plated on LN. The frames are taken at intervals of 4 min. The arrows in the merged images indicate the concentration of NBD-PC in the filopodium and at the edge of the small lamellipodium. The horizontal line across the merged images indicates the tip of the small lamellipodium. Bar, 10 μm. D: Represents the mean fluorescence intensity of NBD-PC and rhodamine-PE in the merged images at all time points depicted in (C). The distribution pattern of lipids in L27 plated on FN and LN was recorded in 15 cells; a representative cell is depicted here.

NBD-PE. In L27 cells plated on FN, NBD-PC had a lower mobility (9.7×10^{-10} cm^2/sec) than NBD-PE (Fig. 6A). We observed two distinct populations of NBD-PE in L27 cells plated on FN, one with higher mobility (77.77×10^{-10} cm^2/sec) and another with lower mobility (13×10^{-10} cm^2/sec). The percent recovery of the fast moving and slow moving NBD-PE populations was 43.68 ± 10.65 and 47.41 ± 7.15, respectively (Table 2). Of the NBD-PE molecules studied, almost half had higher mobility and the other half had lower mobility. NBD-PC and NBD-PE molecules in L27 cells plated on LN had similar mobilities. The recovery curves for NBD-PC and NBD-PE in L27 cells plated on FN or LN nearly matched the mobility patterns for these molecules in cells plated on FN or LN (Fig. 6B). The mobility levels of NBD-PC and NBD-PE in the lamellipodia were significantly higher than those in non-lamellipodial regions of cells plated on FN or LN. Thus, differential mobilities of NBD-PC and NBD-PE were found in the lamellipodia of L27 cells when plated on FN.

Discussion

This study shows that the lateral mobility of the phospholipid component of the plasma membrane is significantly and specifically affected by the substratum the cells adhere to and move on. Nakache et al. (1985) have reported similar observations in human umbilical vein endothelial cells

(HUVEC). However, the specific variation in lateral mobility of PC and PE under various degrees of cell adhesion through specific integrin receptors has not been reported. The way Chol affects lateral mobility of membrane lipids in such a scenario has not been investigated previously. Our study addressed this situation.

A major observation made in this study is that the lateral mobility of PC and PE changed without altering the overall fluidity of the membranes, as measured by DPH polarization (Supplementary Table).

Correlates of PC-FN and FN-integrin interaction

Mobility of PC molecules was low in all the tested cells if they were plated on FN (Fig. 1C). PC mobility was low in parental S180 and D711 cells (both low expressors of α5 integrin) plated on FN. However, PC mobility was significantly lower in L27 cells (high expressor of α5 integrin) plated on FN than in S180 and D711 cells plated on this same substrata. Others have shown that FN molecules spontaneously assemble into fibrillar networks underneath DPPC monolayers (Baneyx and Vogel, 1999) and that FN preferentially adsorbs to the gel phase of PC liposomes, changing the conformation of FN from its inactive, compact state into a more active, open state (Halter et al., 2005). Findings from these reports suggest that FN molecules have specific and strong binding sites for PC molecules, which
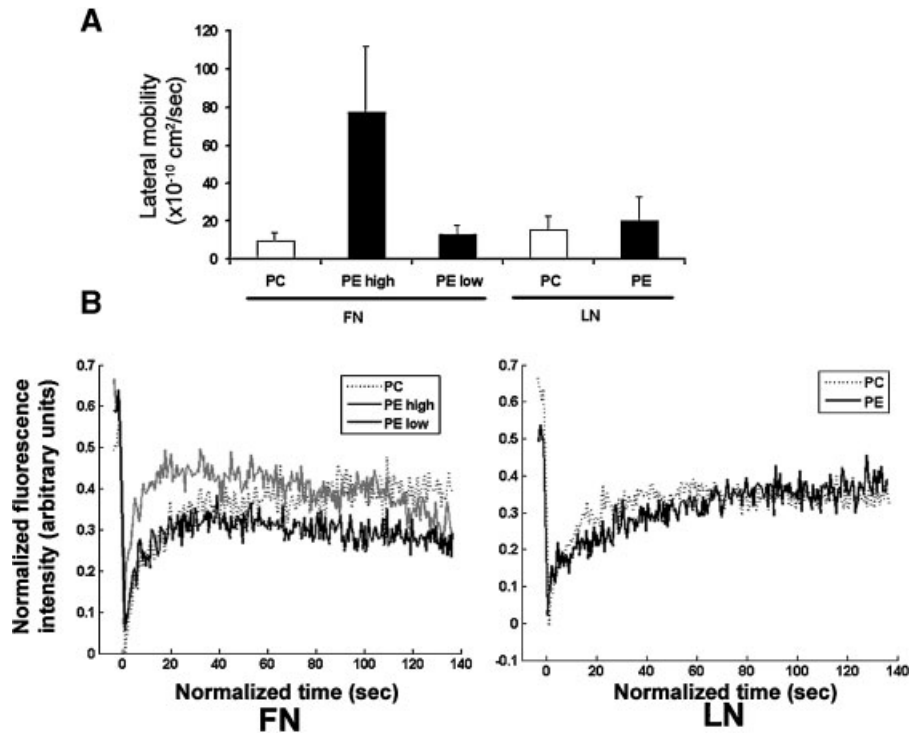
Fig. 6. FRAP analysis of lamellipodial regions of L27 cells plated on various substrata. A: Mean lateral mobility of NBD-PC (white bars) and NBD-PE (black bars) in lamellipodial regions of L27 cells plated on FN and LN. NBD-PE mobility in these cells plated on FN had two distinct populations, one with a higher mobility (PE high, $\cong 7.7 \times 10^{-9}$ cm²/sec) and one with a lower mobility (PE low, $\cong 1.3 \times 10^{-9}$ cm²/sec). B: Representative FRAP recovery curves for NBD-PC (dotted curve), NBD-PE population with high mobility (gray curve), and NBD-PE population with low mobility (black curve) in lamellipodial regions of L27 cells plated on FN (left part). The right part depicts FRAP recovery curves for NBD-PC (dotted curve) and NBD-PE (black curve) in lamellipodial regions of L27 cells plated on LN.

regulate its function. Thus, we hypothesize that strong adhesion of L27 cells overexpressing $\alpha 5$ integrins to FN substrata impairs the mobility of PC in the plasma membrane. We observed low recovery of PC molecules in L27 cells plated on FN (Table 1A), supporting this hypothesis. PC mobility was much less impaired if these cells were plated on LN: we observed high recovery of PC molecules in this case. These findings can be explained by the absence of $\alpha 5$ integrin and $\alpha 4$ integrin interaction with LN. Under these conditions, PC molecules move more freely in the plasma membrane. PE molecules had higher mobility in the three cell types tested when they were plated on FN than when they were plated on LN. However, their mobile fractions were very high in these three cell types plated on both FN and LN (Table 1B), indicating that PE molecules are less specifically associated than PC with FN or LN.

TABLE 2. Percent recovery of NBD-PC or NBD-PE after FRAP experiments in lamellipodial regions of untreated L27 cells plated on FN or LN

Substratum	Phospholipids		
	PC	PE (i)	PE (ii)
FN	80.25 ± 7.7	43.68 ± 10.65	47.41 ± 7.15
LN	57.2 ± 4.4	57.8 ± 17.3	Not applicable

The percent recovery of two populations of NBD-PE with different levels of mobility in the lamellipodia of L27 cells plated on FN is depicted. PE (i) indicates NBD-PE molecules with high lateral mobility and PE (ii) indicates NBD-PE molecules with low lateral mobility in L27 cells plated on FN only. NBD-PE in L27 cells plated on LN did not have these two populations with different levels of lateral mobility.

Our results, shown in Figure 2, clearly demonstrate that interaction of $\alpha 5\beta 1$ integrin with FN plays a direct role in the regulation of PC lateral mobility because when the $\alpha 5\beta 1$ interaction with FN in the ECM is inhibited by RGD peptides the lateral mobility of PC increases. These data also suggest that PC molecules in the membrane could be in closer association with FN, as shown by Halter et al. (2005) and Baneyx and Vogel (1999), when $\alpha 5\beta 1$ integrin is tightly bound to FN. These findings suggest that specific and strong cell adhesion to the ECM through specific integrins affects the behavior of phospholipid molecules in the membrane. This was most clearly shown in cells plated on FN substrata, which binds both PC and $\alpha 5$ integrins in the cell membrane.

Role of cholesterol in PC-PE lateral mobility

PC molecules in L27 cells plated on FN have significantly higher mobility after removal of Chol (Fig. 3A). Chol removal decreases lipid packing order of the membrane (Brown and London, 2000) and impairs adhesion of L27 cells to FN by modulating interaction of $\alpha 5\beta 1$ integrin with FN (Ramprasad et al., 2007). Thus, PC interacts less with FN and is more mobile. Higher PC mobility in Chol-depleted cells may also be caused by removal of constraints for free diffusion of PC molecules. Chol restoration in these cells restores membrane order and lateral packing. Values for PC mobility also reach or slightly surpass levels observed in untreated cells (Fig. 3A).

PC molecules were less mobile in Chol-depleted L27 cells plated on LN than in untreated cells, in contrast with our findings in these cells plated on FN. The explanations for this may be similar to those for changes in lateral mobility of lipid

moieties in the membrane before and after Chol removal, suggested by previous reports. Following Chol depletion, lateral diffusion of DiIC$_{18}$ and *FAST* DiI increased in native hippocampal membranes (Pucadyil and Chattopadhyay, 2006). However, Chol depletion from erythrocyte membranes led to decreased lateral mobility of DiI (Thompson and Axelrod, 1980). In artificial lipid bilayers, with an increase in Chol concentration, diffusion coefficients for DOPC, POPC, and DMPC decreased; however, lateral diffusion of sphingomyelin was not affected (Filippov et al., 2003).

Changes in lateral diffusion due to Chol depletion, in the context of cell adhesion to various matrix proteins, had not been addressed previously. The pattern of changes in PC mobility after Chol depletion in D711 cells, which overexpress α4 integrin, plated on FN and LN was similar to that in L27. However, whereas PC mobility was 4.5 times higher following Chol depletion in D711 cells plated on FN, it was 12.5 times higher in L27 under the same conditions (Fig. 3A). The α4 integrin overexpressed in D711 cells interacts weakly with FN through the LDV motif in the CS-1 region and the REDV motif in the CS-5 region of FN (Pankov and Yamada, 2002). Chol depletion impairs this weak interaction, increasing lateral mobility of PC.

PE mobility changes insignificantly after Chol depletion and restoration in L27, S180, and D711 cells plated on FN or LN (Fig. 3B). PE is an inner bilayer lipid and is probably less affected than PC by Chol changes in the membrane of cells plated on various substrata. There were also insignificant changes in lateral mobility of PC in S180, the parental cell line, plated on FN or LN after Chol depletion and restoration (Fig. 3A). This is possibly due to the weak interaction of the cell with the substrate protein. Cells plated on FN and LN round up after Chol depletion, leading to the depolymerization of actin and weak staining of cortical actin (Ramprasad et al., 2007). The curvature of the cells may also affect the lateral mobility of lipids, similar to the tension-dependent changes in lateral mobility of the lipid di-8-ANEPPS in outer hair cell plasma membranes (Oghalai et al., 2000).

Cell adhesion to matrix and caveolin distribution

The role of caveolin in integrin-mediated cell adhesion and signaling has been reported (Wei et al., 1999). Matrix proteins FN and LN induced differential distributions of caveolar domains when L27 cells overexpressing α5 integrin were plated on them. Chol depletion did not change the distribution of caveolar domains in cells plated on FN and LN. This correlated with our previous report, in which there was no change in the distribution of α5 integrin and paxillin after Chol removal and restoration in L27 cells plated on FN (Ramprasad et al., 2007). The changes in caveolin distribution after Chol depletion in L27 cells plated on PL were very similar to the pattern reported in A431 cells on PL (Claas et al., 2001). It is possible that PC mobility changes after Chol depletion and restoration in L27 cells plated on FN (Fig. 3A) are not associated with domain structures or their distribution in cells adhering to various substrata.

PC/PE distribution and mobility in lamellipodia

There are a few previous reports about the labeling of live cells with fluorescent phospholipids. The transbilayer movement of fluorescent lipid analogs of PS and PE, mediated by ATP, in CHO cells has been reported (Martin and Pagano, 1987). Similarly, Ladha et al. (1997) have shown the differential localization of ODAF and DiIC$_{16}$ in various regions of live spermatozoa. More recently, the localization of NBD-choline and NBD-PC in endoplasmic reticulum of drug sensitive live MCF-7 cells and in the Golgi of drug resistant live MCF-7 cells has been reported (Villa et al., 2005). However, there are no reports about the

imaging and distribution of PC and PE in forming lamellipodia of cells plated on various substrata. PE forms a non-bilayer structure, which facilitates rapid phospholipid transbilayer movement, leading to membrane fusion in model membranes (Ellens et al., 1989). The concentration of PE in the lamellipodia in cells plated on FN may be similar to the redistribution of PE in the cleavage furrow of dividing cells during cytokinesis. Cortical actin filaments disassemble and PE is exposed on the surface in the cleavage furrow during cytokinesis (Emoto et al., 1996; Umeda and Emoto, 1999). Our study shows that PE is exposed on the surface during the formation of lamellipodia, where disassembly and rapid turnover of cortical actin filaments occurs. Thus, PE is a major component of an extending lamellipodium. The formation of filopodia on LN with stress fibers extending to the tips of the filopodia seems to favor PC localization. Though there are no reports about substrate-dependent distribution of lipids in lamellipodia and filopodia, there are a few studies with model membranes, which indicate that LN-derived peptides interact with PC (Alsina et al., 2006).

In a typical lamellipodium formed in L27 cells on FN, there are interactions of α5 integrin and paxillin with FN, the interaction of PC in the outer leaflet of the bilayer with FN and the forces due to the actin meshwork formation of the leading edge. It is possible that polymerizing actin filaments stabilize the position of the components of the plasma membrane at the leading edge, slowing diffusion. Vasanji et al. (2004) have shown that DiIC$_{16}$ diffuses slower in the front of migrating endothelial cells than in the center or back of the cells. No specific substratum was used to measure migration in that study. A similar pattern of slow diffusion of DiIC$_{16}$ has been reported to occur in the leading edge of migrating keratocytes, determined by focal labeling and observation of initial diffusion (FLOID), but not by FRAP analysis (Weisswange et al., 2005). Our study shows that PC mobility in lamellipodia of cells plated on FN was slowed down, but not PE mobility. PC mobility is low because PC is in the outer leaflet of the bilayer, it preferentially adsorbs to FN (Halter et al., 2005), and it is influenced by forces of α5 integrin adhesion to FN and of actin polymerization machinery. However, the mobility of PE, which is in the inner leaflet of the bilayer, is not constrained by these forces as much as PC and thus has high mobility. PE mobility is higher than that of ODAF and NBD-PC even in sperm acrosomes (Christova et al., 2004). PC and PE mobilities were similar in cells plated on LN because the α3β1 and α6β1 receptors moderately expressed in L27 cells led to lower adhesion on LN. Thus, PC and PE were not strongly associated with LN substrate in the lamellipodium.

In summary, we have studied mobility and distribution of PC and PE molecules in cells, which express different types of integrins and exhibit various levels of adhesion and motility on FN and LN. Whereas PC molecules associated strongly with FN in conjunction with α5 integrin interaction with FN, PE molecules associated weakly with any ECM protein. Our findings show that Chol plays an important role in the association of FN with PC in the membranes of α5-integrin-overexpressing cells. ECM proteins affected the distribution of caveolin domains. The differential lipid mobilities may be related to these changes. NBD-PE was preferentially distributed and highly mobile in lamellipodia formed in α5-integrin-overexpressing cells on FN. Thus, PE is an important lipid component of forming lamellipodia. The role and mechanism of F-actin in the preferential distribution of PE have to be elucidated. This study raises further questions about the regulators of lipid-protein interactions in lamellipodia.

Literature Cited

Alsina MA, Ortiz A, Polo D, Comelles F, Reig F. 2006. Synthesis and study of molecular interactions between phosphatidyl choline and two laminin derived peptides hydrophobically modified. J Colloid Interface Sci 294:385–390.

Baneyx G, Vogel V. 1999. Self-assembly of fibronectin into fibrillar networks underneath dipalmitoyl phosphatidylcholine monolayers: Role of lipid matrix and tensile forces. Proc Natl Acad Sci USA 96:12518–12523.

Beauvais A, Erickson CA, Goins T, Craig SE, Humphries MJ, Thiery JP, Dufour S. 1995. Changes in the fibronectin-specific integrin expression pattern modify the migratory behavior of sarcoma S180 cells in vitro and in the embryonic environment. J Cell Biol 128:699–713.

Brown DA, London E. 2000. Structure and function of sphingolipid- and cholesterol-rich membrane rafts. J Biol Chem 275:17221–17224.

Chattopadhyay A. 1990. Chemistry and biology of N-(7-nitrobenz-2-oxa-1, 3-diazol-4-yl)-labeled lipids: Fluorescent probes of biological and model membranes. Chem Phys Lipids 53:1–15.

Christova Y, James P, Mackie A, Cooper TG, Jones R. 2004. Molecular diffusion in sperm plasma membranes during epididymal maturation. Mol Cell Endocrinol 216:41–46.

Claas C, Stipp CS, Hemler ME. 2001. Evaluation of prototype transmembrane 4 superfamily protein complexes and their relation to lipid rafts. J Biol Chem 276:7974–7984.

del Pozo MA, Balasubramanian N, Alderson NB, Kiosses WB, Grande-Garcia A, Anderson RG, Schwartz MA. 2005. Phospho-caveolin-1 mediates integrin-regulated membrane domain internalization. Nat Cell Biol 7:901–908.

Dufour S, Beauvais-Jouneau A, Delouvee A, Thiery JP. 1999. Differential function of N-cadherin and cadherin-7 in the control of embryonic cell motility. J Cell Biol 146:501–516.

Edidin M. 2003. The state of lipid rafts: From model membranes to cells. Annu Rev Biophys Biomol Struct 32:257–283.

Ellens H, Siegel DP, Alford D, Yeagle PL, Boni L, Lis LJ, Quinn PJ, Bentz J. 1989. Membrane fusion and inverted phases. Biochemistry 28:3692–3703.

Emoto K, Umeda M. 2000. An essential role for a membrane lipid in cytokinesis. Regulation of contractile ring disassembly by redistribution of phosphatidylethanolamine. J Cell Biol 149:1215–1224.

Emoto K, Kobayashi T, Yamaji A, Aizawa H, Yahara I, Inoue K, Umeda M. 1996. Redistribution of phosphatidylethanolamine at the cleavage furrow of dividing cells during cytokinesis. Proc Natl Acad Sci USA 93:12867–12872.

Exton JH. 1994. Phosphatidylcholine breakdown and signal transduction. Biochim Biophys Acta 1212:26–42.

Filippov A, Oradd G, Lindblom G. 2003. The effect of cholesterol on the lateral diffusion of phospholipids in oriented bilayers. Biophys J 84:3079–3086.

Fukuhira Y, Kitazono E, Hayashi T, Kaneko H, Tanaka M, Shimomura M, Sumi Y. 2006. Biodegradable honeycomb-patterned film composed of poly(lactic acid) and dioleoylphosphatidylethanolamine. Biomaterials 27:1797–1802.

Gaus K, Le LS, Balasubramanian N, Schwartz MA. 2006. Integrin-mediated adhesion regulates membrane order. J Cell Biol 174:725–734.

Geiger B, Avnur Z, Schlessinger J. 1982. Restricted mobility of membrane constituents in cell-substrate focal contacts of chicken fibroblasts. J Cell Biol 93:495–500.

Gopalakrishna P, Chaubey SK, Manogaran PS, Pande G. 2000. Modulation of $\alpha5\beta1$ integrin functions by the phospholipid and cholesterol contents of cell membranes. J Cell Biochem 77:517–528.

Gopalakrishna P, Rangaraj N, Pande G. 2004. Cholesterol alters the interaction of glycosphingolipid GM3 with alpha5beta1 integrin and increases integrin-mediated cell adhesion to fibronectin. Exp Cell Res 300:43–53.

Groves JT. 2006. Chemistry. Unveiling the membrane domains. Science 313:1901–1902.

Halter M, Antia M, Vogel V. 2005. Fibronectin conformational changes induced by adsorption to liposomes. J Control Release 101:209–222.

Jacobson K, Sheets ED, Simson R. 1995. Revisiting the fluid mosaic model of membranes. Science 268:1441–1442.

Kenworthy AK, Nichols BJ, Remmert CL, Hendrix GM, Kumar M, Zimmerberg J, Lippincott-Schwartz J. 2004. Dynamics of putative raft-associated proteins at the cell surface. J Cell Biol 165:735–746.

Kraft ML, Weber PK, Longo ML, Hutcheon ID, Boxer SG. 2006. Phase separation of lipid membranes analyzed with high-resolution secondary ion mass spectrometry. Science 313:1948–1951.

Kwik J, Boyle S, Fooksman D, Margolis L, Sheetz MP, Edidin M. 2003. Membrane cholesterol, lateral mobility, and the phosphatidylinositol 4,5-bisphosphate-dependent organization of cell actin. Proc Natl Acad Sci USA 100:13964–13969.

Ladha S, James PS, Clark DC, Howes EA, Jones R. 1997. Lateral mobility of plasma membrane lipids in bull spermatozoa: Heterogeneity between surface domains and rigidification following cell death. J Cell Sci 110:1041–1050.

Lentz BR, Moore BM, Barrow DA. 1979. Light-scattering effects in the measurement of membrane microviscosity with Diphenylhexatriene. Biophys J 25:489–494.

Martin OC, Pagano RE. 1987. Transbilayer movement of fluorescent analogs of phosphatidylserine and phosphatidylethanolamine at the plasma membrane of cultured cells. Evidence for a protein-mediated and ATP-dependent processes. J Biol Chem 262:5890–5898.

Munro S. 2003. Lipid rafts: Elusive or illusive? Cell 115:377–388.

Nakache M, Schreiber AB, Gaub H, McConnell HM. 1985. Heterogeneity of membrane phospholipid mobility in endothelial cells depends on cell substrate. Nature 317:75–77.

Oghalai JS, Zhao HB, Kutz JW, Brownell WE. 2000. Voltage- and tension-dependent lipid mobility in the outer hair cell plasma membrane. Science 287:658–661.

Pande G. 2000. The role of membrane lipids in regulation of integrin functions. Curr Opin Cell Biol 12:569–574.

Pankov R, Yamada KM. 2002. Fibronectin at a glance. J Cell Sci 115:3861–3863.

Parton RG, Hanzal-Bayer M, Hancock JF. 2006. Biogenesis of caveolae: A structural model for caveolin-induced domain formation. J Cell Sci 119:787–796.

Pucadyil TJ, Chattopadhyay A. 2006. Effect of cholesterol on lateral diffusion of fluorescent lipid probes in model membranes. Chem Phys Lipids 143:11–21.

Ramprasad OG, Srinivas G, Sridhar Rao K, Joshi P, Thiery JP, Dufour S, Pande G. 2007. Changes in cholesterol levels in the plasma membrane modulate cell signaling and regulate cell adhesion and migration on fibronectin. Cell Motil Cytoskeleton 64:199–216.

Razani B, Woodman SE, Lisanti MP. 2002. Caveolae: From cell biology to animal physiology. Pharmacol Rev 54:431–467.

Simons K, Toomre D. 2000. Lipid rafts and signal transduction. Nat Rev Mol Cell Biol 1:31–39.

Singer SJ, Nicolson GL. 1972. The fluid mosaic model of the structure of cell membranes. Science 175:720–731.

Thompson NL, Axelrod D. 1980. Reduced lateral mobility of a fluorescent lipid probe in cholesterol-depleted erythrocyte membrane. Biochim Biophys Acta 597:155–165.

Tournier JF, Lopez A, Tocanne JF. 1989. Effect of cell substratum on lateral mobility of lipids in the plasma membrane of vascular endothelial cells. Exp Cell Res 181:105–115.

Umeda M, Emoto K. 1999. Membrane phospholipid dynamics during cytokinesis: Regulation of actin filament assembly by redistribution of membrane surface phospholipid. Chem Phys Lipids 101:81–91.

Vasanji A, Ghosh PK, Graham LM, Eppell SJ, Fox PL. 2004. Polarization of plasma membrane microviscosity during endothelial cell migration. Dev Cell 6:29–41.

Villa AM, Caporizzo E, Papagni A, Miozzo L, Del BP, Grilli MD, Amboldi N, Fazio F, Doglia SM, Giglioni B. 2005. Choline and phosphatidylcholine fluorescent derivatives localization in carcinoma cells studied by laser scanning confocal fluorescence microscopy. Eur J Cancer 41:1453–1459.

Wei Y, Yang X, Liu Q, Wilkins JA, Chapman HA. 1999. A role for caveolin and the urokinase receptor in integrin-mediated adhesion and signaling. J Cell Biol 144:1285–1294.

Weisswange I, Bretschneider T, Anderson KI. 2005. The leading edge is a lipid diffusion barrier. J Cell Sci 118:4375–4380.

Yechiel E, Barenholz Y, Henis YI. 1985. Lateral mobility and organization of phospholipids and proteins in rat myocyte membranes. Effects of aging and manipulation of lipid composition. J Biol Chem 260:9132–9136.

Yguerabide J, Schmidt JA, Yguerabide EE. 1982. Lateral mobility in membranes as detected by fluorescence recovery after photobleaching. Biophys J 40:69–75.

Zachowski A. 1993. Phospholipids in animal eukaryotic membranes: Transverse asymmetry and movement. Biochem J 294:1–14.